

This is a repository copy of *Investigation of the  $\Delta n = 0$  selection rule in Gamow-Teller transitions : The  $\beta$ -decay of  $^{207}\text{Hg}$ .*

White Rose Research Online URL for this paper:  
<https://eprints.whiterose.ac.uk/146351/>

Version: Published Version

---

## Article:

Berry, T. A., Podolyák, Zs, Carroll, R. J. et al. (59 more authors) (2019) Investigation of the  $\Delta n = 0$  selection rule in Gamow-Teller transitions : The  $\beta$ -decay of  $^{207}\text{Hg}$ . Physics Letters, Section B: Nuclear, Elementary Particle and High-Energy Physics. pp. 271-275. ISSN 0370-2693

<https://doi.org/10.1016/j.physletb.2019.04.039>

---

## Reuse

This article is distributed under the terms of the Creative Commons Attribution (CC BY) licence. This licence allows you to distribute, remix, tweak, and build upon the work, even commercially, as long as you credit the authors for the original work. More information and the full terms of the licence here:  
<https://creativecommons.org/licenses/>

## Takedown

If you consider content in White Rose Research Online to be in breach of UK law, please notify us by emailing [eprints@whiterose.ac.uk](mailto:eprints@whiterose.ac.uk) including the URL of the record and the reason for the withdrawal request.



# Investigation of the $\Delta n = 0$ selection rule in Gamow-Teller transitions: The $\beta$ -decay of $^{207}\text{Hg}$

T.A. Berry<sup>a,\*</sup>, Zs. Podolyák<sup>a</sup>, R.J. Carroll<sup>a</sup>, R. Lică<sup>b,c</sup>, H. Grawe<sup>d</sup>, N.K. Timofeyuk<sup>a</sup>, T. Alexander<sup>a</sup>, A.N. Andreyev<sup>e</sup>, S. Ansari<sup>f</sup>, M.J.G. Borge<sup>b,g</sup>, J. Creswell<sup>h</sup>, C. Fahlander<sup>j</sup>, L.M. Fraile<sup>i</sup>, H.O.U. Fynbo<sup>k</sup>, W. Gelletly<sup>a</sup>, R.-B. Gerst<sup>l</sup>, M. Górska<sup>d</sup>, A. Gredley<sup>l</sup>, P. Greenlees<sup>m</sup>, L.J. Harkness-Brennan<sup>l</sup>, M. Huyse<sup>n</sup>, S.M. Judge<sup>o</sup>, D.S. Judson<sup>l</sup>, J. Konki<sup>m,p,b</sup>, J. Kurcewicz<sup>b</sup>, I. Kuti<sup>q</sup>, S. Lalkovski<sup>a</sup>, I. Lazarus<sup>h</sup>, M. Lund<sup>k</sup>, M. Madurga<sup>b</sup>, N. Mărginean<sup>c</sup>, R. Mărginean<sup>c</sup>, I. Marroquin<sup>g</sup>, C. Mihai<sup>c</sup>, R.E. Mihai<sup>c</sup>, E. Nácher<sup>g</sup>, S. Nae<sup>c</sup>, A. Negret<sup>c</sup>, C. Niță<sup>c,r</sup>, R.D. Page<sup>l</sup>, S. Pascu<sup>c</sup>, Z. Patel<sup>a</sup>, A. Perea<sup>g</sup>, V. Pucknell<sup>h</sup>, P. Rahkila<sup>m</sup>, E. Rapisarda<sup>b</sup>, P.H. Regan<sup>a,o</sup>, F. Rotaru<sup>c</sup>, C.M. Shand<sup>a</sup>, E.C. Simpson<sup>s</sup>, Ch. Sotty<sup>c,n</sup>, S. Stegemann<sup>f</sup>, T. Stora<sup>b</sup>, O. Tengblad<sup>g</sup>, A. Turturica<sup>c</sup>, P. Van Duppen<sup>n</sup>, V. Vedia<sup>i</sup>, R. Wadsworth<sup>e</sup>, P.M. Walker<sup>a</sup>, N. Warr<sup>f</sup>, F. Wearing<sup>l</sup>, H. De Witte<sup>n</sup>

<sup>a</sup> Department of Physics, University of Surrey, Guildford, GU2 7XH, United Kingdom

<sup>b</sup> CERN, Physics Department, 1211 Geneva 23, Switzerland

<sup>c</sup> H. H. Hulubei National Institute for Physics and Nuclear Engineering, Bucharest, Romania

<sup>d</sup> GSI Helmholtzzentrum für Schwerionenforschung GmbH, Planckstrasse 1, 64291 Darmstadt, Germany

<sup>e</sup> Department of Physics, University of York, York YO10 5DD, N Yorkshire, United Kingdom

<sup>f</sup> Institut für Kernphysik der Universität zu Köln, Zùlpicher Str. 77, 50937 Köln, Germany

<sup>g</sup> Instituto de Estructura de la Materia, CSIC, Serrano 113 bis, E-28006 Madrid, Spain

<sup>h</sup> STFC, Daresbury Laboratory, Warrington, WA4 4AD, United Kingdom

<sup>i</sup> Grupo de Física Nuclear & IPARCOS, FAMN, Universidad Complutense de Madrid, CEI Moncloa, 28040 Madrid, Spain

<sup>j</sup> Department of Physics, Lund University, S-22100, Lund, Sweden

<sup>k</sup> Department of Physics and Astronomy, Aarhus University, DK-8000 Aarhus, Denmark

<sup>l</sup> Department of Physics, Oliver Lodge Laboratory, University of Liverpool, Liverpool, United Kingdom

<sup>m</sup> Department of Physics, PO Box 35 (YFL), FI-40014 University of Jyväskylä, Finland

<sup>n</sup> KU Leuven, Instituut voor Kern- en Stralingsfysica, Celestijnenlaan 200D, 3001 Leuven, Belgium

<sup>o</sup> National Physical Laboratory, Teddington, Middlesex, TW11 0LW, United Kingdom

<sup>p</sup> Helsinki Institute of Physics, University of Helsinki, FIN-00014 Helsinki, Finland

<sup>q</sup> Institute of Nuclear Research of the Hungarian Academy of Sciences, 4026 Debrecen, Hungary

<sup>r</sup> School of Computing, Engineering and Mathematics, University of Brighton, Brighton BN2 4GJ, United Kingdom

<sup>s</sup> Department of Nuclear Physics, Australian National University, Canberra, Australian Capital Territory 2601, Australia

## ARTICLE INFO

### Article history:

Received 15 January 2019

Received in revised form 12 March 2019

Accepted 11 April 2019

Available online 24 April 2019

Editor: D.F. Geesaman

## ABSTRACT

Gamow-Teller  $\beta$  decay is forbidden if the number of nodes in the radial wave functions of the initial and final states is different. This  $\Delta n = 0$  requirement plays a major role in the  $\beta$  decay of heavy neutron-rich nuclei, affecting the nucleosynthesis through the increased half-lives of nuclei on the astrophysical  $r$ -process pathway below both  $Z = 50$  (for  $N > 82$ ) and  $Z = 82$  (for  $N > 126$ ). The level of forbiddenness of the  $\Delta n = 1$   $\nu 1g_{7/2} \rightarrow \pi 0g_{7/2}$  transition has been investigated from the  $\beta^-$  decay of the ground state of  $^{207}\text{Hg}$  into the single-proton-hole nucleus  $^{207}\text{Tl}$  in an experiment at the ISOLDE Decay Station. From statistical observational limits on possible  $\gamma$ -ray transitions depopulating the  $\pi 0g_{7/2}^{-1}$  state in  $^{207}\text{Tl}$ , an

\* Corresponding author.

E-mail address: t.berry@surrey.ac.uk (T.A. Berry).

upper limit of  $3.9 \times 10^{-3}\%$  was obtained for the probability of this decay, corresponding to  $\log ft > 8.8$  within a 95% confidence limit. This is the most stringent test of the  $\Delta n = 0$  selection rule to date.

© 2019 The Authors. Published by Elsevier B.V. This is an open access article under the CC BY license (<http://creativecommons.org/licenses/by/4.0/>). Funded by SCOAP<sup>3</sup>.

The theory of  $\beta$  decay was developed by Fermi in 1934 [1]. In its modern form it is derived from the standard model of the electroweak interaction [2,3]. Based on the orbital angular momentum  $L$  carried by the  $\beta$  particle and neutrino, the  $\beta$  decay is classified as allowed ( $L = 0$ ), first-forbidden ( $L = 1$ ) and so on. The so-called forbidden transitions are hindered, but not completely suppressed. The selection rules for allowed  $\beta$  decay are total angular momentum change  $\Delta I = 0, \pm 1$  and no parity change between the initial (decaying) and final (populated) states. In contrast, first-forbidden transitions have  $\Delta I = 0, \pm 1, \pm 2$  and a change in parity. These are the selection rules which can be found in textbooks. However, in the case of allowed  $\beta$  transitions, there is one additional rule: the number of nodes,  $n$ , in the radial wave functions of the decaying and populated states must be equal.

The  $\Delta n = 0$  selection rule plays a major role in heavy neutron-rich nuclei. The single-particle shell-model orbitals for the  $N > 126$ ,  $Z < 82$  region ('south-east' of  $^{208}\text{Pb}$ ) are shown in Fig. 1. The several pairs of  $\Delta n = 1$ ,  $\Delta l = 0$  orbitals are indicated. If the  $\Delta n = 0$  selection rule is strictly obeyed,  $\beta$  decay between them is forbidden, resulting in longer lifetimes. The greatest impact is on nuclei where the Fermi level lies high above  $N = 126$  and/or much below  $Z = 82$ , e.g. nuclei on the astrophysical  $r$ -process pathway, influencing the nucleosynthesis of heavy elements. On the other hand, this selection rule has little effect on isotopes which are proton-rich or close to the stability line, making the experimental investigation of its validity difficult. We explored the  $\nu 1g_{9/2} \rightarrow \pi 0g_{7/2}$  transition in the  $\beta$  decay of  $^{207}\text{Hg}$  in a high-statistics experiment performed at CERN-ISOLDE. In this letter we provide the most stringent test of the  $\Delta n = 0$  selection rule to date.

The  $\beta$ -decay probabilities are characterised by  $\log ft$  values, where  $f$  is the Fermi function and  $t$  is the partial half-life. For allowed ( $L = 0$ ) decay  $ft$  can be written as [5]:

$$ft \times (B_F + B_{GT}) = \frac{\pi^2 \hbar^7 \ln(2)}{2m_e^5 c^4} \quad (1)$$

where  $B_F$  and  $B_{GT}$  are the Fermi (total spin of the electron and antineutrino is  $S = 0$ ) and the Gamow-Teller ( $S = 1$ ) reduced transition probabilities, and are proportional to the  $|M_{fi}^F|^2$  and  $|M_{fi}^{GT}|^2$  matrix elements respectively. These in turn are summed over the single-particle matrix elements. These single-particle matrix elements are equal to zero if the number of radial nodes in the wave function,  $n$ , changes between the initial and final states. The  $\Delta n = 0$  selection rule applies for both Fermi and Gamow-Teller transitions. For details see ref. [6].

Far from the  $N = Z$  line, Fermi decays are isospin-forbidden ( $\Delta T \neq 0$ ), so considering Gamow-Teller transitions only one obtains [5–7]:

$$ft = \frac{6147}{1.62 \frac{1}{2I_i+1} |\langle \Psi_f || \tau_{\pm} \sigma || \Psi_i \rangle|^2} \quad (2)$$

where  $\tau_{\pm}$  is the isospin step operator converting either a proton to a neutron or a neutron to a proton respectively,  $\sigma$  is the Pauli spin operator, and  $\Psi_{i,f}$  are the initial and final total nuclear wave functions. From the form of the operators the selection rules of  $\Delta I = 0, \pm 1$  with no parity change follow. The matrix element is related to the overlap  $\mathcal{L}$  of the initial and final state wave functions:

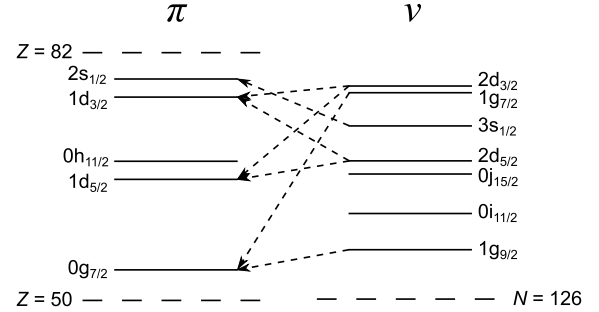


Fig. 1. Shell model orbitals for  $50 < Z < 82$  and  $126 < N < 184$ . The ordering and energy spacing of the orbitals are taken from the experimental level schemes of  $^{207}\text{Tl}$  and  $^{209}\text{Pb}$  respectively [4]. Arrows link proton-neutron pairs which satisfy the  $\Delta I = 0$ ,  $\Delta n = 1$  condition.

$$\mathcal{L} = \int_0^\infty \Psi_i(r) \Psi_f(r) r^2 dr. \quad (3)$$

For  $\Delta n \neq 0$ , if the Hamiltonians are identical (i.e. spin-orbit and Coulomb effects are ignored) then the radial wave functions are orthogonal, and  $\mathcal{L} = 0$ . The assessment of the  $\Delta n = 0$  selection rule requires a good understanding of both initial and final states. This is achieved in the vicinity of the doubly magic nuclei, when the wave functions can be given in terms of a few single-particle components.

According to our knowledge, the  $\Delta n = 0$  selection rule was verified for a single case: that of the  $\beta$  decay of  $^{209}\text{Tl}$  into  $^{209}\text{Pb}$  [8]. The present case of the  $^{207}\text{Hg} \rightarrow ^{207}\text{Tl}$  decay provides a more stringent test, due to larger spin-coupling coefficients and the stronger contributions of the relevant single-particle orbitals to the overall wave functions.

The  $^{207}\text{Hg}$  ground state has an expected spin-parity of  $9/2^+$ , corresponding to a neutron in the  $\nu 1g_{9/2}$  orbital above the  $N = 126$  magic number. The daughter nucleus  $^{207}\text{Tl}$  is one proton hole away from doubly magic  $^{208}\text{Pb}$ . It exhibits clear single-particle behaviour with the  $7/2^+$   $\pi 0g_{7/2}^{-1}$  hole state at an energy of 3474(6) keV [9]. This state has been populated in a number of particle transfer experiments [10–14]. In the present letter we examine the  $\nu 1g_{9/2} \rightarrow \pi 0g_{7/2}$   $\beta$  decay, allowed in terms of spin-parities but forbidden by the  $\Delta n = 0$  selection rule.

The  $\beta$  decay of  $^{207}\text{Hg}$  into  $^{207}\text{Tl}$  has been studied at the ISOLDE Decay Station (IDS). A molten lead target was bombarded with 1.4 GeV protons.  $^{207}\text{Hg}$  ions were extracted at 30 kV from the VD5 FEBIAD source [15], separated by the General Purpose Separator (GPS) and collected on the tape at IDS. The average implantation yield was  $4.8(2) \times 10^4$  pps. The dominant beam contaminant was  $^{206}\text{Hg}$ , with a presence of around 0.6 times that of  $^{207}\text{Hg}$ . However, with a  $Q_\beta = 1.31(2)$  MeV and few  $\gamma$  transitions [16] it does not impact the current results.  $\beta$  decay and  $\gamma$  rays were detected by three plastic scintillators in a close configuration and an array of high-purity germanium (HPGe) detectors, respectively. The HPGe array consisted of four Canberra Clover detectors, arranged at equal angular separation at a backward angle, and a Miniball [17] cluster detector along the beam axis. The full detector set-up had a gamma-ray add-back efficiency of 22% at 100 keV and 4% at 2.6 MeV, and a  $\beta$ -particle efficiency of  $\sim 30\%$ . Extension of the efficiency calibration up to 2.6 MeV was performed by using the

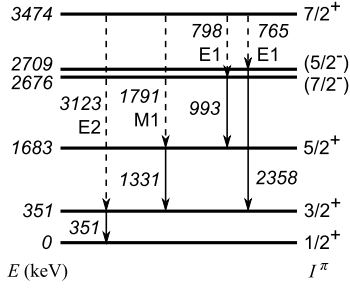


**Fig. 2.** Partial level scheme of  $^{207}\text{Tl}$ . Transitions expected to de-populate the state at 3474(6) keV are drawn with dashed arrows. Observed transitions, used as gates for coincidence spectra, are drawn with solid arrows.

relative intensities of the 583 keV and 2614 keV peaks from the  $\beta$  decay of  $^{208}\text{Tl}$  [18], measured on a separate GPS mass setting during the same experiment.

The analysis of this experiment revealed the level scheme of  $^{207}\text{Tl}$  up to an energy of 3.94 MeV [19]. It is in good agreement with the previously established scheme [20], and contains a number of newly-observed states and transitions. The level scheme is now complete and balanced. A partial level scheme, showing levels and transitions used in this analysis, is shown in Fig. 2.

The four lowest-energy states correspond to shell model single-proton-hole states: the  $\pi 2s_{1/2}^{-1}$  ground state; the  $\pi 1d_{3/2}^{-1}$  state at 351 keV; the isomeric  $\pi 0h_{11/2}^{-1}$  state at 1348 keV (not shown on Fig. 2); and the  $\pi 1d_{5/2}^{-1}$  state at 1683 keV. At 2676 and 2709 keV lie the pair of states corresponding to the coupling of the  $3^{-}$  octupole vibrational phonon to the ground state [20]. Above these, up to an energy of 3.8 MeV, lie a number of  $(7/2, 9/2, 11/2)^{-}$  states, some of which result from octupole coupling with the  $\pi 1d_{3/2}^{-1}$  state and others involving other negative-parity particle-hole excitations.

No transitions into or out of the  $\pi 0g_{7/2}^{-1}$  proton-hole state at 3474(6) keV were observed. As the decay of this state was never observed [9], we used theoretical considerations to evaluate which states it would populate (see Fig. 2). The M3 and M2 transitions to the  $1/2^{+}$  ground state and  $11/2^{-}$  isomeric state, respectively, would be extremely weak and so are ignored. The high-energy 3123(6) keV E2 transition to the  $3/2^{+}$  first excited state is expected to be dominant. This is a  $g_{7/2} \rightarrow d_{3/2}$  transition connecting  $\Delta j = \Delta l = 2$  states. The 1791(6) keV M1+E2 transition to the  $5/2^{+}$  state may be of comparable strength, although the M1 decay in this  $g_{7/2} \rightarrow d_{5/2}$  transition is  $l$ -forbidden. The next two excited states at 2676 keV and 2709 keV have spin-parity  $(7/2^{-})$  and  $(5/2^{-})$ , respectively [20]. Many E1 transitions, some connecting equivalent single-particle and octupole states, have been observed in nearby nuclei [16,21–24]. Measured  $B(E1)$  transition strengths are in the range of  $10^{-3}$ – $10^{-5}$  W.u. Therefore we adopt an upper limit of  $B(E1) = 10^{-3}$  W.u. for the possible 798(6) keV and the 765(6) keV transitions. The typical E1 strength is an order of magnitude smaller than this upper limit.

Most of the observed states between 2709 and 3474 keV have spin-parity  $(5/2, 7/2, 9/2)^{-}$  [9]. Due to the lower energies of the possible E1 transitions into these states, the branching ratios from the  $\pi g_{7/2}^{-1}$  state should be smaller. In order to have comparable intensity to the 3123 keV E2 transition they need to have an unrealistically high strength of  $B(E1) > 0.05$  W.u. Therefore these transitions are not considered. The properties of the four most probable depopulating transitions, including the estimated branching ratios, are given in Table 1. The latter are based on shell-model values of  $B(M1)$  and  $B(E2)$  transition strengths. These calculations assume pure  $(0g_{7/2}, 1d, 2s)$  proton hole states and standard effective E2 proton charge of  $1.5e$  [25–27]. In order to obtain the

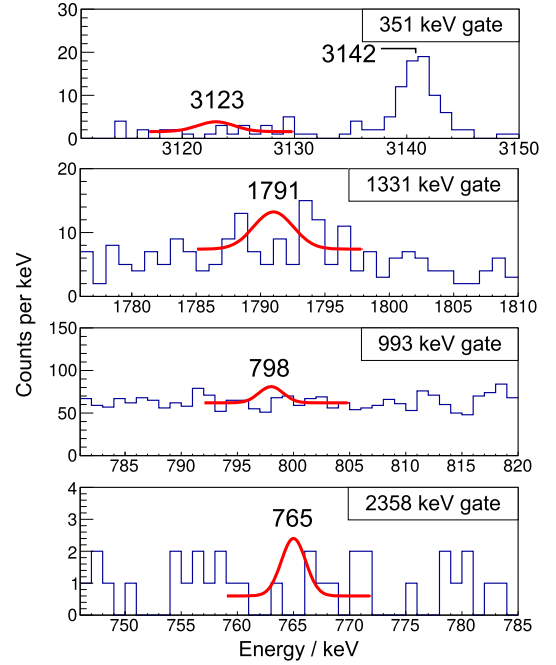


**Fig. 3.**  $\beta$ -gated  $\gamma\gamma$  coincidence spectra for transitions expected to de-populate the 3474(6) keV state in  $^{207}\text{Tl}$ . Fit lines show calculated upper limits on unobserved peak intensity, using an  $N = 2$  (95% confidence) statistical limit. The peak with energy 3142 keV in coincidence with the 351 keV transition (top spectrum) implies the existence of a state at 3493 keV, discussed in the text.

strength of the  $l$ -forbidden  $g_{7/2} \rightarrow d_{5/2}$  M1 transition, a  $g_p[s \times Y_2]$  tensor term into the effective operator [28,29] was introduced. Adopting the  $0g_{7/2}-1d_{5/2}$  vs.  $1d_{3/2}-2s_{1/2}$  scaling calculated for a  $^{132}\text{Sn}$  core in the same model space [29], and considering the radial overlaps of the involved orbitals, the  $B(M1)$  value of 0.0041 W.u. was obtained.

The most stringent non-observation limits were obtained from  $\beta\gamma\gamma$  coincidence data. Where a transition is not observed, an upper limit on the intensity can be deduced from the uncertainty in the relevant background area,  $I_\gamma < N\sqrt{2A}$ .  $N$  is the number of standard deviations used, and  $A$  is the background area below the expected peak. The  $\gamma\gamma$  coincidences used are indicated in Fig. 2, and the resulting coincidence spectra for the four different gating transitions are shown in Fig. 3. The extracted intensity limits, for  $N = 2$  (95% confidence limit), are given in Table 1. The limits cover all energies within  $2\sigma$  (12 keV) of the central energy. As shown in Table 1, the highest-energy transition is expected to dominate. Assuming a lower limit of 90% for the branching ratio of the 3123 keV transition, we would obtain a maximum possible population of the 3474 keV  $7/2^{+}$  state of  $1.2 \times 10^{-3}$  leading to the final result  $\log ft > 9.3$ . However, we can reduce our reliance on the shell model calculations by considering any branching ratios between all four transitions. In this case, the maximum possible population of the 3474 keV  $7/2^{+}$  state is  $3.9 \times 10^{-3}$  leading to the final result  $\log ft > 8.8$ .

The shell model calculations performed for further interpretation are based on the Kuo-Herling interaction [30,31] in the  $pp$  and  $hh$  channels, and proton-neutron two-body matrix elements (TBMEs) from a H7B G-matrix [32,33] in the  $ph$ ,  $hp$  and cross-shell channels relative to  $^{208}\text{Pb}$ . The combined interaction KHH7B (or PBKH7) in a  $\pi(0g_{7/2}, 1d, 2s, 0h_{11/2})^{-1}(0h_{9/2}, 1f, 2p, 0i_{13/2})$  and  $\nu(0h_{9/2}, 1f, 2p, 0i_{13/2})^{-1}(0i_{11/2}, 1g, 2d, 3s, 0j_{15/2})$  model space is provided by the OXBASH package [34] as PBALL.



**Table 1**

Experimentally obtained  $I_\gamma$  intensity limits presented as a  $\gamma$ -ray emission probability per hundred  $\beta$  decays of the  $^{207}\text{Hg}$  parent nucleus, along with shell-model calculated transition strengths and corresponding branching ratios.

$E_\gamma$ (keV)	$I_{\gamma, \text{exp}}$ (%)	$\sigma L$	$B(\sigma L)_{\text{the}}$ (W.u.)	$B_{R, \text{the}}$ (%)
3123(6)	$< 1.07 \times 10^{-3}$	E2	2.07	92.3
1791(6)	$< 3.86 \times 10^{-3}$	M1+E2	0.0041 (M1) 0.23 (E2)	1.9
798(6)	$< 3.21 \times 10^{-3}$	E1	$\ll 10^{-3}$	$\ll 3.1$
765(6)	$< 1.43 \times 10^{-3}$	E1	$\ll 10^{-3}$	$\ll 2.7$

The initial and final wave functions are:

$$\Psi_i(^{207}\text{Hg}; 9/2^+) = \phi_C \cdot \sum_j \alpha_j (\pi j^{-2})_{0+} (\nu 1g_{9/2}) \quad (4)$$

$$\Psi_f(^{207}\text{Tl}; 7/2^+) = \phi_C \cdot (\pi 0g_{7/2}^{-1}) \quad (5)$$

where  $\phi_C$  is the  $^{208}\text{Pb}$  core and  $\sum_j \alpha_j (\pi j^{-2})_{0+}$  is the wave function of two proton holes outside the core. The resulting reduced Gamow-Teller matrix element is given by the equation

$$\langle \Psi_f | \tau_\pm \sigma | \Psi_i \rangle = \sqrt{6} \hat{j}_i \hat{j}_f \mathcal{L} \alpha_{7/2} W(1, 1/2, j_f, l; 1/2, j_i) \quad (6)$$

where the notation  $\hat{j} = \sqrt{2j+1}$  is used. The Racah coefficient  $W$  is equal to 0.19245 for this decay.  $\alpha_{7/2}^2$  is the probability that there are two holes in the  $\pi 0g_{7/2}$  orbital in the ground state of  $^{207}\text{Hg}$ . The shell model calculation in the  $\pi h$ - $\nu p$  space yields  $\alpha_{7/2} = 0.095$ .  $\mathcal{L} = \langle \nu 1g_{9/2} | \pi 0g_{7/2} \rangle$  is the overlap integral between the specified single particle states.

From this information we obtain a limit  $|\mathcal{L}| < 0.019$ . This is a stricter limit than that obtained from the  $\beta$  decay of  $^{209}\text{Tl}$  for the overlap of the  $\nu 3s_{1/2}$  and  $\pi 2s_{1/2}$  orbitals [8]. The reasons are the lower experimental  $\log ft > 8.35$  limit in the case of  $^{209}\text{Tl}$ , and the lower  $\nu 3s_{1/2}^{-2}$  contribution to the  $^{209}\text{Tl}$  ground state ( $\alpha_{1/2} = 0.05$  using the same shell model calculation).

The overlap integral  $\mathcal{L}$  is very sensitive to the difference between the neutron and proton well radii. By calculating the value of the integral using a Woods-Saxon potential, using known proton and neutron separation energies and fixing the surface thickness and neutron radius parameter to  $a = 0.65$  fm and  $r_v = 1.25 \times A^{1/3}$  fm respectively, the result suggests that the  $0g_{7/2}$  proton well radius parameter is between 0% and 1.5% larger than the  $1g_{9/2}$  neutron orbital parameter. Knowledge of these parameters is important in models of transfer reactions and neutron skin calculations.

So far we have not considered mixing in the 3474(6) keV state. Indeed, spectroscopic factor measurements suggest that the  $\pi 0g_{7/2}^{-1}$  orbital is dominant but with large mixing [12]. The other components might be populated by allowed  $\beta$  decay. Another  $7/2^+$  state with  $\pi h_{11/2}^{-1} \times 3^-$  configuration is expected  $\sim 500$  keV above the  $g_{7/2}$  state, but in this case the phonon coupling is not stretched. Due to vector coupling coefficients the mixing is expected to be small [35,36] and is not considered. More important are certain two-particle-three-hole ( $2p-3h$ ) excitations. Such states are obtained if in  $^{207}\text{Hg}$  a neutron in a  $N < 126$  orbital decays into a  $Z > 82$  orbital. In these  $2p-3h$  final states both the proton and neutron cores are broken. Shell-model calculations were performed, allowing hole states  $\pi(g_{7/2}, d, s_{1/2}, h_{11/2})$  and  $\nu(h_{9/2}, f, p, i_{13/2})$  to be excited to selected particle states  $\pi(h_{9/2}, f_{7/2}, i_{13/2})$  and  $\nu(g_{9/2}, i_{11/2})$ , respectively. The high-spin states of  $^{207}\text{Tl}$  [37] were well-reproduced. The yrast  $7/2^+$  state is predicted to be 78%  $\pi g_{7/2}^{-1}$ . In this approach all relevant Gamow-Teller transitions  $\nu(h_{9/2}, f, i) \rightarrow \pi(h_{9/2}, f_{7/2}, i_{13/2})$ , are accounted for. The Gamow-Teller strength into the  $7/2^+$  state was calculated. Considering a quenching factor of 0.56 [38], a population of this state at

a level of  $8 \times 10^{-3}\%$  is predicted, corresponding to  $\log ft = 8.53$ . In conclusion, the theoretically predicted population of the yrast  $7/2^+$  state is around twice the experimentally determined upper limit for the excited state at 3474(6) keV. An uncertainty of 50% in the population predicted by the shell model would reconcile the observed and predicted values.

While no peak was observed in the 351 keV  $\gamma\gamma$  coincidence spectrum at the expected energy of 3123 keV, a small peak at 3142 keV (shown in Fig. 3) implies the existence of a state with an energy of 3494 keV. This lies three standard deviations away from 3474(6) keV, and with no other supporting transitions a spin-parity assignment is not possible. Nevertheless, in the case that the state at 3494 keV is the  $7/2_1^+$  state previously placed at 3474(6) keV, this would imply an observed  $\beta$ -feeding intensity of  $8(1) \times 10^{-3}\%$  and  $\log ft = 8.53(9)$ . This is exactly the value predicted by the shell model for the population of the yrast  $\pi 0g_{7/2}$ -dominated  $7/2^+$  state. It would still imply that the  $\Delta n = 0$  selection rule is observed, as the observed population of this state from the  $\beta$  decay of  $^{207}\text{Hg}$  would be fully accounted for by the  $2p-3h$  mixing.

In the absence of the  $\Delta n = 0$  selection rule, the lifetimes of the  $^{207}\text{Hg}$  and  $^{209}\text{Tl}$  nuclei would be shorter. Assuming  $\log ft$  equal to the modal average of the empirical distribution for allowed transitions [39], the Gamow-Teller transitions would take approximately 5% and 20% of the decay intensity into  $^{207}\text{Tl}$  and  $^{209}\text{Pb}$  respectively, shortening the half-life of  $^{207}\text{Hg}$  by around 7% and that of  $^{209}\text{Tl}$  by around 20%. The effects are much larger for extremely neutron-rich heavy nuclei. Close to  $^{208}\text{Pb}$  the contributions of the relevant wave functions in the mother/daughter nuclei are very low, with amplitudes  $\alpha_{1/2} = 0.05$  for  $^{209}\text{Tl}$  and  $\alpha_{7/2} = 0.095$  for  $^{207}\text{Hg}$ . These increase dramatically for extremely neutron-rich nuclei, when either exploring deeper into the proton shell below  $Z = 82$  or extending further into  $N > 126$  (see the ordering of orbitals on Fig. 1). For example, the  $r$ -process path is predicted to cross the  $Z = 82$  line at around neutron number  $N \sim 160$ –170 [40]. In this region, just below  $Z = 82$ , the  $\Delta n = 0$  selection rule will have an impact on the lifetimes by forbidding the  $\nu 3s_{1/2} \rightarrow \pi 2s_{1/2}$  and  $\nu 2d_{3/2} \rightarrow \pi 1d_{3/2}$  Gamow-Teller transitions. The effect of this selection rule for the decay of  $N = 126$   $r$ -process waiting-point nuclei is negligible because of the minimal contribution from  $N > 126$  orbitals. The same selection rule also affects nuclei ‘south-east’ of  $^{132}\text{Sn}$  [41] due to the existence of  $\Delta n = 1$ ,  $\Delta l = 0$  neutron-proton orbital pairs in the region of  $N > 82$  and  $Z < 50$ . Experimental investigation of the forbiddenness in this mass region is an interesting possibility but remains challenging due to the large  $Q_\beta$  values.

The  $\beta$  decay of  $^{207}\text{Hg}$  was studied and a search was made for  $\gamma$ -rays following the  $n$ -forbidden  $\nu 1g_{9/2} \rightarrow \pi 0g_{7/2}$  Gamow-Teller  $\beta$  decay. From the non-observation of this decay, a  $\log ft > 8.9$  limit at 95% confidence level was deduced. This is the most stringent test of the  $\Delta n = 0$  rule to date, and suggests that the selection rule is indeed obeyed. The rule has implications for the decays of the neutron-rich nuclei in both the  $N > 82$ ,  $Z < 50$  and  $N > 126$ ,  $Z < 82$  regions. In the latter region, the lifetimes of nuclei on the astrophysical  $r$ -process path are considerably increased, affecting the nucleosynthesis of heavy elements.

## Acknowledgements

Support from the European Union seventh framework through ENSAR contract no. 262010, the Science and Technology Facilities Council through grants ST/P005314/1, ST/L005743/1 and ST/J000051/1 (UK), the MINECO projects FPA2015-64969-P, FPA2015-65035-P and FPA2017-87568-P (Spain), FWO-Vlaanderen (Belgium), GOA/2015/010 (BOF KU Leuven), the Excellence of Science programme (EOS-FWO), and the Interuniversity Attraction Poles

Programme initiated by the Belgian Science Policy Office (BriX network P7/12) is acknowledged. ZsP acknowledges support by the ExtreMe Matter Institute EMMI at the GSI Helmholtzzentrum für Schwerionenforschung, Darmstadt, Germany. PHR and SMJ acknowledge support from the UK Department for Business, Energy and Industrial Strategy via the National Measurement Office.

## References

- [1] E. Fermi, *Z. Phys.* **88** (1934) 161.
- [2] S.L. Glashow, J. Iliopoulos, L. Maiani, *Phys. Rev. D* **2** (1970) 1285.
- [3] H. Georgi, S.L. Glashow, *Phys. Rev. Lett.* **32** (1974) 438.
- [4] A. Heusler, et al., *Phys. Rev. C* **93** (2016) 054321.
- [5] A. Bohr, B.R. Mottelson, *Nuclear Structure*, vol. I, W. A. Benjamin, New York, 1969, p. 411.
- [6] J. Suhonen, *From Nucleons to Nucleus: Concepts of Microscopic Nuclear Theory*, 1st ed., Springer-Verlag, Berlin, 2007, pp. 157–204.
- [7] M. Tanabashi, et al., *Phys. Rev. D* **98** (2018) 030001.
- [8] V.M. Datar, et al., *Phys. Rev. C* **22** (1980) 1787.
- [9] F.G. Kondev, S. Lalkovski, *Nucl. Data Sheets* **112** (2011) 707.
- [10] P. Barnes, et al., *Phys. Rev. C* **1** (1970) 228.
- [11] E.R. Flynn, et al., *Nucl. Phys. A* **279** (1977) 394.
- [12] P. Grabmayr, et al., *J. Phys. G* **18** (1992) 1753.
- [13] I. Bobeldijk, et al., *Phys. Lett. B* **356** (1995) 13.
- [14] M. Hunyadi, et al., *Nucl. Phys. A* **731** (2004) 49.
- [15] T. Stora, *Nucl. Instrum. Methods Phys. Res. B* **317** (2013) 402.
- [16] F.G. Kondev, *Nucl. Data Sheets* **109** (2008) 1527.
- [17] N. Warr, et al., *Eur. Phys. J. A* **49** (2013) 40.
- [18] M.J. Martin, *Nucl. Data Sheets* **108** (2007) 1583.
- [19] T.A. Berry, PhD thesis, University of Surrey, 2019.
- [20] B. Jonson, et al., *CERN* **81-09** (1981) 640.
- [21] C.J. Chiara, F.G. Kondev, *Nucl. Data Sheets* **111** (2010) 141.
- [22] F.G. Kondev, *Nucl. Data Sheets* **101** (2004) 521.
- [23] M. Kadi, et al., *Phys. Rev. C* **61** (2000) 034307.
- [24] J. Chen, F.G. Kondev, *Nucl. Data Sheets* **126** (2015) 373.
- [25] S.J. Steer, et al., *Phys. Rev. C* **84** (2011) 044313.
- [26] S.J. Steer, et al., *Phys. Rev. C* **78** (2008) 061302.
- [27] E. Caurier, M. Rejmund, H. Grawe, *Phys. Rev. C* **67** (2003) 054310.
- [28] F. Petrovich, *Nucl. Phys. A* **203** (1973) 65.
- [29] B.A. Brown, et al., *Phys. Rev. C* **71** (2005) 044317.
- [30] T.T.S. Kuo, G.H. Herling, U.S. Naval Research Laboratory report 2258, 1971.
- [31] G.H. Herling, T.T.S. Kuo, *Nucl. Phys. A* **181** (1972) 113.
- [32] A. Hosaka, K.I. Kubo, H. Toki, *Nucl. Phys. A* **444** (1985) 76.
- [33] E.K. Warburton, B.A. Brown, *Phys. Rev. C* **43** (1991) 602.
- [34] B.A. Brown, *Oxbash for Windows PC*, MSU-NSCL report 1289, 2004.
- [35] A. Bohr, B.R. Mottelson, *Nuclear Structure*, vol. II, W. A. Benjamin, New York, 1975, p. 418.
- [36] M. Rejmund, et al., *Eur. Phys. J. A* **8** (2000) 161.
- [37] E. Wilson, et al., *Phys. Lett. B* **747** (2015) 88.
- [38] E. Caurier, et al., *Rev. Mod. Phys.* **77** (2005) 427.
- [39] B. Singh, et al., *Nucl. Data Sheets* **84** (1998) 487.
- [40] M. Arnould, et al., *Phys. Rep.* **450** (2007) 97.
- [41] J. Taprogge, et al., *Eur. Phys. J. A* **52** (2016) 347.